Published in final edited form as:
Hepatology. 2002 August ; 36(2): 284–296. doi:10.1053/jhep.2002.34432.

Regulation of Ca^{2+} Signaling in Rat Bile Duct Epithelia by Inositol 1,4,5-Trisphosphate Receptor Isoforms

Keiji Hirata[1], **Jean-François Dufour**[2], **Kazunori Shibao**[1], **Roy Knickelbein**[1], **Allison F. O'Neill**[1], **Hans-Peter Bode**[3], **Doris Cassio**[4], **Marie V. St-Pierre**[5], **Nicholas F. LaRusso**[6], **M. Fatima Leite**[7], and **Michael H. Nathanson**[1]

[1]Department of Internal Medicine, Yale University School of Medicine, New Haven, CT [2]Department of Clinical Pharmacology, University of Bern, Bern, Switzerland [3]Department of Gastroenterology, University of Bern, Bern, Switzerland [4]INSERM U442, University Paris XI, Paris, France [5]Department of Clinical Pharmacology, University of Zürich, Zürich, Switzerland [6]Department of Medicine, Mayo Clinic, Rochester, MN [7]Department of Physiology and Biophysics, UFMG, Belo Horizonte, Brazil

Abstract

Cytosolic Ca^{2+} (Ca_i^{2+}) regulates secretion of bicarbonate and other ions in the cholangiocyte. In other cell types, this second messenger acts through Ca^{2+} waves, Ca^{2+} oscillations, and other subcellular Ca^{2+} signaling patterns, but little is known about the subcellular organization of Ca^{2+} signaling in cholangiocytes. Therefore, we examined Ca^{2+} signaling and the subcellular distribution of Ca^{2+} release channels in cholangiocytes and in a model cholangiocyte cell line. The expression and subcellular distribution of inositol 1,4,5-trisphosphate ($InsP_3$) receptor ($InsP_3R$) isoforms and the ryanodine receptor (RyR) were determined in cholangiocytes from normal rat liver and in the normal rat cholangiocyte (NRC) polarized bile duct cell line. Subcellular Ca^{2+} signaling in cholangiocytes was examined by confocal microscopy. All 3 $InsP_3R$ isoforms were expressed in cholangiocytes, whereas RyR was not expressed. The type III $InsP_3R$ was the most heavily expressed isoform at the protein level and was concentrated apically, whereas the type I and type II isoforms were expressed more uniformly. The type III $InsP_3R$ was expressed even more heavily in NRC cells but was concentrated apically in these cells as well. Adenosine triphosphate (ATP), which increases Ca^{2+} via $InsP_3$ in cholangiocytes, induced Ca^{2+} oscillations in both cholangiocytes and NRC cells. Acetylcholine (ACh) induced apical-to-basal Ca^{2+} waves. In conclusion, Ca^{2+} signaling in cholangiocytes occurs as polarized Ca^{2+} waves that begin in the region of the type III $InsP_3R$. Differential subcellular localization of $InsP_3R$ isoforms may be an important molecular mechanism for the formation of Ca^{2+} waves and oscillations in cholangiocytes. Because Ca_i^{2+} is in part responsible for regulating ductular secretion, these findings also may have implications for the molecular basis of cholestatic disorders.

Cytosolic Ca^{2+} (Ca_i^{2+}) regulates a wide range of functions in the liver. One way in which Ca_i^{2+} simultaneously regulates multiple cell functions is through spatial and temporal Ca_i^{2+} signaling patterns, such as Ca_i^{2+} waves and oscillations. For example, localized subplasmalemmal increases in Ca_i^{2+} direct secretion,[1-3] whereas Ca_i^{2+} gradients direct cell

Address reprint requests to: Michael H. Nathanson, M.D., Ph.D., Section of Digestive Diseases, Room 1080 LMP, Yale University School of Medicine, 333 Cedar St., New Haven, CT 06520-8019. michael.nathanson@yale.edu; fax: 203-785-4306..

motion.[4-7] Temporal Ca_i^{2+} signaling patterns such as oscillations also can regulate cell functions, including gene expression[8,9] and secretion.[10] Although Ca_i^{2+} oscillations can be induced in cholangiocytes,[11] it is unknown whether Ca_i^{2+} waves or other subcellular Ca_i^{2+} signaling patterns also occur in this cell type.

The formation of Ca_i^{2+} waves in polarized epithelia is believed to depend largely on intracellular Ca^{2+} stores rather than plasma membrane Ca^{2+} channels, because neither the orientation nor the speed of such waves is altered in Ca^{2+}-free media.[12] The 2 intracellular Ca^{2+} channels principally responsible for Ca_i^{2+} signaling are the inositol 1,4,5-trisphosphate ($InsP_3$) receptor ($InsP_3R$) and the ryanodine receptor (RyR). It was previously believed that RyRs regulate Ca_i^{2+} signaling only in myocytes, whereas $InsP_3Rs$ regulate Ca_i^{2+} signaling in nonexcitable epithelia. However, many cell types express both RyR and $InsP_3R$,[13,14] including polarized epithelia.[15,16] Moreover, there are multiple isoforms of both of these receptors, each of which displays distinct functional properties.[17-20] Thus, the formation of Ca_i^{2+} waves likely depends not only on the expression and subcellular distribution of RyRs and $InsP_3Rs$, but on the distribution of individual isoforms of each of these receptors as well. Here we examine the expression and subcellular distribution of these Ca^{2+} release channels in cholangiocytes from rat liver and in normal rat cholangiocyte (NRC) cells, a polarized rat cholangiocyte cell line used as a model for cholangiocyte function.[21]

Materials and Methods

Animals and Materials

Male Sprague-Dawley rats (250-300 g; Camm Research Lab Animals, Wayne, NJ) were used for all animal studies. Acetylcholine (ACh), adenosine triphosphate (ATP), propidium iodide, deoxyribonuclease, hyaluronidase, bovine serum albumin, penicillin-streptomycin, and insulin were obtained from Sigma Chemical Co. (St. Louis, MO). Fluo-4 and fura-2 in acetoxymethyl ester form, Pluronic F-127, and rhodamine-conjugated phalloidin were obtained from Molecular Probes (Eugene, OR). SuperScript II ribonuclease H^- reverse transcriptase, colcemid, minimal essential medium (MEM), α-MEM, Liebowitz 15 (L-15), gentamicin, and other tissue culture reagents were from Gibco BRL (Life Technologies AG, Basel, Switzerland). Collagen-coated flasks were from Becton Dickinson, Bedford, MA. RQ1 ribonuclease-free deoxyribonuclease was from Promega (Wallisellen, Switzerland). Pronase was from Calbiochem (La Jolla, CA).

Antibodies

Each $InsP_3R$ isoform was labeled using isoform-specific antibodies. Type I $InsP_3R$ antibodies were from affinity-purified specific rabbit polyclonal antiserum directed against the 19 C-terminal residues of the mouse type I $InsP_3R$[22] and were produced by Research Genetics (Huntsville, AL). Type II $InsP_3R$ antibodies were from affinity-purified specific rabbit polyclonal antiserum directed against the 18 C-terminal residues of the rat type II $InsP_3R$[23] and were kindly provided by Richard Wojcikiewicz (SUNY, Syracuse, NY). A commercially available monoclonal antibody was used to label the N-terminal region of the human type III $InsP_3R$[17] (Transduction Laboratories, Lexington, KY).

Cell Isolation and Cell Culture

Cholangiocytes and isolated rat bile duct units were isolated from normal rat liver as described previously.[11] Briefly, rats were anesthetized with pentobarbital sodium (50 mg/kg body wt intraperitoneally) and then their livers were perfused with Ca^{2+}- and Mg^{2+}-free Hank's buffer/0.019% ethylenediaminetetraacetic acid followed by Hank's buffer containing 0.05%

collagenase (Boehringer Mannheim Biochemicals, Indianapolis, IN). The portal tissue residue was then either cut into strips for Ca_i^{2+} measurements or processed further to obtain isolated cholangiocytes. For Ca_i^{2+} studies, the long wavelength lipophilic dye 1,1′-dioctadecyl-3,3,3′, 3′-tetramethylindodicarbocyanine perchlorate (DiD; Molecular Probes) was first injected into the common bile duct to facilitate identification of cholangiocytes within portal strips (see below). To isolate cholangiocytes, the tissue was finely minced, digested further, and then filtered through nylon screens (Tetko, Lancaster, NY). The suspension was subjected to centrifugation in a Percoll density gradient.[11] Cells banding at densities 1.060 to 1.075 were collected, elutriated, and then used for Western blot analysis. This resulted in more than 10^7 cells per liver, ~70% of which stained positive for γ-glutamyl transpeptidase and more than 90% of which were viable by trypan blue exclusion.

The NRC cell line was maintained in culture for separate studies. This polarized cell line is derived from normal rat cholangiocytes.[21] Cells were maintained in culture on collagen in cholangiocyte growth medium.[21]

Immunoblot Analysis

Protein concentration of cell homogenate was determined as described.[24] Cholangiocyte or NRC cell proteins were separated by electrophoresis using a 5% polyacrylamide gel and transferred to nitrocellulose membranes. The membranes were blocked at 4°C overnight and probed for 2 hours with the primary antibody. The antibody against $InsP_3R$ isoform I was used at a dilution of 1:60, the antibody against $InsP_3R$ isoform II was used at a dilution of 1:100, and the antibody against $InsP_3R$ isoform III was used at a dilution of 1:1,000. Peroxidase-conjugated secondary antibodies were from Pierce (Rockford, IL). The membranes were washed, incubated for 1 hour with peroxidase-conjugated secondary antibody immunoglobulin G anti-rabbit (1: 1,000) or anti-mouse (1:3,000), and shown by enhanced chemiluminescence (Amersham, Arlington Heights, IL). For quantitative analyses, immunoblotting was performed on samples of rat cholangiocytes or NRC cells along with positive controls containing known concentrations of $InsP_3R$ isoforms.[23] For each immunoblot, type I, II, and III $InsP_3R$ immunoreactivity was then quantified using a BioRad GS-700 imaging densitometer (Richmond, CA). $InsP_3R$ isoform protein expression in cholangiocytes and controls was compared directly to yield the relative abundance of each isoform in cholangiocytes.[23] Specifically, the ratio of cholangiocyte or NRC cell band intensity divided by control cell band intensity was multiplied by the $InsP_3R$ isoform concentration in the control cells or tissue to obtain the $InsP_3R$ isoform concentration in cholangiocytes or NRC cells. Cerebellum was used as a standard for type I $InsP_3R$ (129.6 ng/10 μg protein), whole liver was used for type II $InsP_3R$ (0.65 ng/10 μg protein), and the RIN cell line was used for type III $InsP_3R$ (14.1 ng/10 μg protein).[23] The relationship between band intensity and amount of $InsP_3R$ loaded onto gels was linear over the range seen in the present study.

Confocal Immunofluorescence Microscopy

Immunochemistry was performed on 4-μm-thick frozen sections of rat liver hilum containing bile ducts or on NRC cells grown on coverslips. Specimens were fixed by cold acetone, methanol, or 3% formaldehyde followed by methanol permeabilization. After blocking steps, specimens were labeled with primary antibody, rinsed with phosphate-buffered saline, and incubated with Alexa 488 – or Alexa 568 – conjugated secondary antibody (Molecular Probes). Bile ducts also were stained with rhoda-mine-conjugated phalloidin to label actin, which is most concentrated beneath the plasma membrane,[12,15,25] or with propidium iodide to stain the nucleus.[26] For negative control studies, tissue was incubated with secondary antibodies but anti-$InsP_3R$ (primary) antibodies were omitted. Specimens were examined using a Zeiss LSM 510 confocal microscope equipped with a krypton/argon laser (Thornwood, NY). To ensure

specificity of staining, images were obtained using confocal machine settings that detected no fluorescence in negative controls. NRC cells were examined using either a Zeiss Axioskop microscope or a BioRad Microradiance AG-2 confocal system.

RNA Isolation and Reverse Transcription

Total RNA was extracted as described.[27] The concentration of RNA collected from the cholangiocytes or NRC cells was determined by absorbance at 260 nm, and the quality was controlled by running an aliquot on a 1% agarose form-aldehyde gel.

Polymerase Chain Reaction Analyses

Two types of polymerase chain reaction (PCR) analyses were performed. Reverse transcription (RT) PCR was performed to determine whether cholangiocytes or NRC cells express RyR, whereas real-time quantitative PCR was performed to examine relative amounts of $InsP_3R$ isoforms in cholangiocytes and NRC cells. For RT-PCR, 5 μg of total RNA was treated with RQ1 ribonuclease-free deoxyribonuclease and reverse transcribed by the SuperScript II ribonuclease H^- reverse transcriptase with an oligo(dT) primer. Two control complementary DNA reactions were performed; RNA but no reverse transcriptase was added (RNA control) in one, and no RNA was added (DNA control) in the other. PCR amplification was performed using a PTC-100 automated thermocycler (MJ Research, Inc., Watertown, MA) using 2 μL of the first strand complementary DNA reaction, 150 pmol of each degenerate primer, 50 μmol/L deoxynucleoside triphosphates, 2.5 U AmpliTaq DNA polymerase in 10 mmol/L Tris-HCl (pH 8.3) containing 50 mmol/L KCl, and 2.5 mmol/L $MgCl_2$ in a total volume of 100 μL. Following hot start (2 minutes at 94°C), the samples were subjected to 30 cycles of 45 seconds at 94°C, 1 minute at 50°C, and 1 minute at 72°C. This was followed by a final extension at 72°C for 10 minutes. The degenerate primers were designed to amplify a 530 – base pair product from the 3′ region of all 3 known RyRs.[15] In selected experiments, primers were designed to probe for each of the 3 RyR isoforms. For those studies, TCAAGCGGAAGGTTCTGGA was the sequence used for rRyR1-20-5′, TGACGGATGAAAGGATGGTG was used for rRyR1-352-3′, CATGGATAAGGTCGCACTGGA was used for rRyR2-75-5′, CGAGCTGTTTGCCATTATGG was used for rRyR2-364-3′, TTGGACAAAAATGCCCTGGA was used for rRyR3-88-5′, and GGTCTTAAAGCCCATGGCAATA was used for rRyR3-324-3′. Each PCR product was analyzed by agarose gel electrophoresis.

Real-time quantitative PCR analysis of $InsP_3R$ iso-forms and glyceraldehyde-3-phosphate dehydrogenase was performed with a PE Applied Biosystems 7700 Sequence Detector (Perkin Elmer, Shelton, CT) as described previously.[28] Complementary DNA was amplified in a 50 μL volume containing 25 μL of the 2× TaqMan Universal PCR Master Mix (Perkin Elmer), 100 nmol/L probe, and 300 nmol/L of each primer. After a denaturing step of 10 minutes at 95°C, 40 cycles were performed: 95°C for 15 seconds and 60°C for 1 minute. The mathematical analysis of the results was performed as recommended by the manufacturer.

Ca_i^{2+} Measurements

Confocal microscopy was used to measure Ca_i^{2+} in cholangiocytes because cells were within thick segments of the bile duct or in isolated bile duct units. Epifluorescence microscopy was used to monitor Ca_i^{2+} in NRC cell monolayers. For confocal imaging, DiD (25 μmol/L) and the Ca^{2+} dye fluo-4/acetoxymethyl ester (18 μmol/L) were coinjected into the common bile duct, and then bile duct segments were isolated as previously described. The bile duct segments were observed using a BioRad MRC 1024 confocal imaging system. Tissue was excited at 647 nm and observed at more than 680 nm to identify DiD-labeled cholangiocytes, and then Ca_i^{2+} was

monitored by exciting the specimen at 488 nm and detecting emission signals greater than 515 nm. Images were obtained at a rate of 1 image per second to identify hormone-responsive cells,[26] and then confocal line scanning[29,30] was performed to identify the speed and direction of Ca_i^{2+} waves. Cells were observed using a 20×, 0.75 NA objective (zoom factor, 5), resulting in a spatial resolution of 0.20 μm/pixel and a temporal resolution of 6 milliseconds. Increases in Ca_i^{2+} were expressed as percent increase in fluo-4 fluorescence intensity.[11,26,29] Velocities of Ca_i^{2+} waves were determined from the rate at which fluorescence increases moved along the scan line.[29,30]

For NRC cell studies, cells were loaded with fura-2 (5 μmol/L) and then observed using a Zeiss Axiovert 135 inverted microscope. Measurements of Ca_i^{2+} were performed using a Zeiss Attofluor imaging system. Cells were excited at 334 and 380 nm, and emission signals greater than 520 nm were observed with an intensified CCD camera. Ca_i^{2+} was calculated from the excitation ratio R according to the following equation[31]:

$$Ca_i^{2+} = (R - R_{min}) / (R_{max} - R) \times K_d \times (Sf2/Sb2).$$

Calibrations were performed using standards containing Ca^{2+}-saturated and Ca^{2+}-free fura-2, respectively. This yielded R_{max}, R_{min}, Sf2, and Sb2. A value of 224 nmol/L was used for K_d. NRC cells were measured before confluence, when the cells were present in large (>20 cells) islands. The traces shown represent values from regions of interest covering approximately one cell each.

Statistics

Results are expressed as mean ± SD. Comparisons between groups were made using Student's *t* test, and a *P* value less than .05 indicates a significant difference.

Results

Expression of $InsP_3Rs$ and RyR in Cholangiocytes and NRC Cells

Expression of all 3 $InsP_3R$ isoforms was detected in cholangiocytes by quantitative measurement of messenger RNA (mRNA). Using this approach, 40.8% of $InsP_3R$ mRNA was for the type I isoform, 38.0% was for type II, and 21.2% was for type III (Fig. 1). Expression of all 3 $InsP_3R$ isoforms was also detected in NRC cells by this approach. The relative mRNA distribution of the $InsP_3R$ in NRC cells was 20% for the type I isoform, 13% for type II, and 67% for type III (Fig. 2). This finding is consistent with the observation that expression of the type III $InsP_3R$ is increased in cell lines relative to what is observed in the corresponding native tissue.[32] In contrast to the $InsP_3R$, RyR expression could not be detected in cholangiocyte mRNA using RT-PCR (Fig. 3). RT-PCR was also performed with NRC cell mRNA using primers specific for each of the 3 known isoforms of the RyR (Fig. 4). RyR-2 and RyR-3 were absent from NRC cells. A faint band for RyR-1 was detected after 35 cycles, suggesting that this isoform also is not expressed or is expressed only minimally. Together, these findings suggest that the $InsP_3R$ is the principal intracellular Ca^{2+} release channel in cholangiocytes as well as NRC cells.

Immunoblots were performed to determine whether cholangiocytes express all 3 $InsP_3R$ isoforms at the protein level (Fig. 5). Determination of the relative protein level of each isoform is complicated by the fact that each iso-form-specific antibody has a different affinity for its epitopes. Therefore, to estimate relative protein levels, quantitative immunoblots for each isoform were performed along with blots from tissues that express known concentrations of

each $InsP_3R$ isoform.[23] Densitometric quantification of immunoreactivity that comigrated with each positive control showed that cholangiocytes expressed 1.37 ± 0.17 ng of the type III $InsP_3R$ per 10 μg cell protein (mean ± SD) but only 0.12 ± 0.12 ng/10 μg protein of type I and only 0.15 ± 0.07 ng/10 μg protein of type II (Fig. 5D). Thus, most $InsP_3Rs$ in cholangiocytes (84%) are the type III isoform, with lesser amounts of types I (7%) and II (9%). This confirms that all 3 $InsP_3R$ isoforms are expressed in cholangiocytes; however, in contrast to the findings of our PCR studies, these results suggest that the type III $InsP_3R$ is the predominant isoform at the protein level. Immunoblots were also performed to determine whether NRC cells express all 3 $InsP_3R$ isoforms at the protein level. NRC cells expressed 7.6 ± 0.5 ng/10 μg protein of the type III $InsP_3R$, but neither the type I nor type II isoform could be detected (Fig. 6). This suggests that, at the protein level, nearly all $InsP_3Rs$ in NRC cells are the type III isoform.

Subcellular Localization of $InsP_3R$ Isoforms

The subcellular distribution of the type I, II, and III $InsP_3Rs$ was investigated in cholangiocytes and NRC cells by confocal immunofluorescence histochemistry. Rat liver sections were labeled with isoform-specific $InsP_3R$ antibodies and colabeled with rhodamine-conjugated phalloidin to identify the actin network beneath apical and basolateral membrane or propidium iodide to identify the nucleus of cholangiocytes (Fig. 7). Type I and II $InsP_3Rs$ were uniformly distributed throughout the cytosol (Fig. 7A and B). Although type III $InsP_3R$ immunofluorescence was also seen throughout the cytosol, labeling was most intense in the apical region (Fig. 7D and E). No labeling was seen in negative control tissues stained with secondary but not primary antibodies (Fig. 7C and F). The mean apical and basolateral fluorescence intensity of each isoform was determined to quantify these observations (Fig. 7G). The ratio of apical/basolateral fluorescence was 1.10 ± 0.04 for the type I $InsP_3R$ and 1.14 ± 0.04 for type II but 2.63 ± 0.31 for type III ($P < .0002$ relative to the type I and II isoforms; n = 8 measurements for each group). This suggests that the subcellular pattern of distribution of the type III $InsP_3R$ differs from that of the type I and II $InsP_3Rs$ in cholangiocytes. Confocal immunofluorescence was also used to examine the subcellular distribution of the type III $InsP_3R$ in NRC cells. Optical sections obtained near the apical membrane showed a diffuse pattern of $InsP_3R$ labeling (Fig. 8A-C), whereas sections obtained in the basolateral region showed minimal labeling (Fig. 8D-F). As with cholangiocytes, NRC cells thus express the type III $InsP_3R$ to a greater extent in the apical region. Thus, cholangiocytes and NRC cells share certain key features in the expression and subcellular distribution of $InsP_3R$ isoforms, although there are differences as well.

Ca^{2+} Signaling in Cholangiocytes and NRC Cells

To examine Ca_i^{2+} signaling, cells were stimulated with ATP, which is known to increase Ca_i^{2+} through activation of $InsP_3Rs$ in cholangiocytes.[11] NRC cells were exposed to ATP apically, because only the apical side of these cells is exposed and because both cholangiocytes[33] and NRC cells[34] express apical P2Y receptors that link to $InsP_3$ formation. Apical exposure of NRC cells to extracellular ATP (1-100 μmol/L) elicited an immediate increase in Ca_i^{2+} followed by Ca_i^{2+} oscillations (Fig. 9A and B). These oscillations terminated quickly on removal of the agonist. For comparison, the effect of ATP on Ca_i^{2+} signaling was examined in individual cholangiocytes within isolated bile duct units (Fig. 9C). ATP induced Ca_i^{2+} oscillations in cholangiocytes, similar to what has been observed in cholangiocytes previously[11] and in NRC cells here. Because of technical constraints, the current studies compared Ca_i^{2+} signals induced by stimulation of apical ATP receptors in NRC cells with basolateral ATP receptors in cholangiocytes. Although the response of cholangiocytes to ATP is attenuated when the cells are stimulated basolaterally rather than apically, cholangiocytes nonetheless express the same subtypes of P2Y ATP receptors on their apical and basolateral

membrane.[33] These findings thus show that there are functional as well as structural similarities in Ca_i^{2+} signaling between cholangiocytes and NRC cells.

Subcellular Ca^{2+} Signaling Patterns in cholangiocytes

To determine the relationship between the distribution of $InsP_3R$ isoforms and subcellular Ca_i^{2+} signaling patterns, fluo-4–loaded cholangiocytes were examined by confocal line scanning microscopy.[29,30] This imaging approach was used because it is well suited to detect subcellular Ca_i^{2+} signals, which typically occur on a millisecond timescale.[35,36] Because confocal line scanning microscopy of polarized epithelia requires the apical-to-basal axis of the cells to be within the focal plane,[29,30,37] we examined Ca_i^{2+} signaling in cholangiocytes within microdissected segments of intrahepatic bile ducts. However, Ca_i^{2+} signaling in NRC cells could not be examined by this approach because their apical-to-basal axis is perpendicular to the plane of focus. Individual cholangiocytes within intrahepatic bile duct segments were double labeled by retrograde injection of fluo-4 plus DiD before microdis-section to facilitate identification of the cells (Fig. 10). Bile duct segments then were stimulated with either ACh or ATPγS, both of which cause an $InsP_3$-mediated increase in Ca_i^{2+} in this cell type.[11] The nonhydrolyzable form of ATP was used here because nucleotides otherwise are rapidly hydrolyzed at the basolateral membrane of cholangiocytes.[33] ACh (100 μmol/L) caused an increase in Ca_i^{2+} throughout the cholangiocyte. The increase in Ca_i^{2+} began in the apical region and then spread rapidly (22.5 ± 9.3 μm/s; n = 40) to the basolateral region (Fig. 11). Both the direction and speed of this Ca_i^{2+} wave were unchanged in Ca^{2+}-free medium (21.5 ± 7.9 μm/s; n = 8; $P > .35$). Progressive, apical-to-basal increases in Ca_i^{2+} also were observed in cholangiocytes stimulated with ATPγS (Fig. 11E). These findings suggest that $InsP_3$-mediated Ca_i^{2+} signals in cholangiocytes begin in the apical region and then spread as polarized, apical-to-basal Ca_i^{2+} waves.

Discussion

There are 3 isoforms of the $InsP_3R$, and it was previously reported that the type III isoform is expressed in cholangiocytes.[28] Here we report that cholangiocytes actually express all 3 isoforms of the $InsP_3R$ but in different amounts and subcellular distributions. Specifically, the type III isoform was most concentrated apically, whereas the other 2 isoforms were distributed more uniformly throughout the cytosol. Although quantitative PCR studies suggested that each isoform is expressed to a similar extent, immunoblotting instead suggested that the type III isoform is expressed most heavily. There are several possible reasons for this apparent discrepancy. First, mRNA levels do not always reflect protein levels. Second, cholangiocyte mRNA could have been contaminated with mRNA from hepatocytes, which predominantly express the type I and II isoforms.[23,28] Finally, errors may have been introduced by our method of estimating $InsP_3R$ protein levels. However, our immunofluorescence examination of bile ducts plus the quantitative PCR studies of NRC cells together support the conclusion that the type III $InsP_3R$ is indeed the most heavily expressed iso-form. It was previously reported based on quantitative PCR studies that cholangiocytes lose the type III $InsP_3R$ but gain type II $InsP_3R$ after bile duct ligation.[28] In hepatocytes, the type II $InsP_3R$ comprises 80% of the total pool of $InsP_3R$ and the remainder is the type I isoform.[23] Therefore, the profile of $InsP_3R$ isoforms in cholangiocytes becomes similar to hepatocytes after bile duct ligation. Together, these findings suggest that the expression and subcellular distribution of $InsP_3Rs$ in cholangiocytes is more similar to what is found in NRC cells than in cholangiocytes following bile duct ligation.

The current findings also show that Ca_i^{2+} signals begin in the apical region of cholangiocytes, even though $InsP_3$ presumably is generated basolaterally when cells are stimulated with ACh. There are several observations that may explain this finding. First, the range of $InsP_3$ is up to 25 μm in cytosol,[38] so it is feasible for $InsP_3$ to act at a site different from where it is produced. Second, we observed that $InsP_3$Rs are more concentrated in the apical region of cholangiocytes, and InsP -mediated Ca_i^{2+} signals may begin in regions where the $InsP_3$R is clustered.[39] Finally, Ca_i^{2+} signals in cholangiocytes begin in the region where the type III $InsP_3$R is concentrated. This is consistent with the idea that the type III isoform of the $InsP_3$R acts as a molecular trigger for Ca_i^{2+} signals, because Ca^{2+} released from this isoform stimulates further Ca^{2+} release in a positive feedback fashion.[17] This isoform is localized to the apex of a number of epithelia in addition to cholangiocytes, including pancreatic and salivary acinar cells[40-42] and the nonpigmented epithelium of the ciliary bilayer of the eye,[25] and the apical region serves as the initiation site for Ca_i^{2+} waves in each of these cell types. Furthermore, hormone-induced Ca_i^{2+} waves spread from the apical to the basal pole in each of these cell types, as it does in cholangiocytes. However, there are at least 2 different mechanisms by which polarized Ca_i^{2+} waves may spread. In acinar cells, all 3 $InsP_3$R isoforms are apical,[40-42] whereas the RyR is basolateral.[15] The $InsP_3$R is required for apical initiation of the Ca_i^{2+} signal, whereas the RyR is needed for this signal to spread into the basolateral region.[30,37,43,44] In contrast, nonpigmented epithelium cells express only the type III $InsP_3$R apically and express the type I $InsP_3$R basolaterally.[25] Thus, the type I $InsP_3$R rather than the RyR is responsible for the spread of Ca_i^{2+} waves into the basolateral region in that cell type. Because cholangiocytes express type I and II $InsP_3$Rs in the baso-lateral region and do not express the RyR, the molecular basis for Ca_i^{2+} waves in cholangiocytes seems similar to what occurs in nonpigmented epithelium cells.

How does the current study increase our understanding of bile duct cell function? Evidence from other polarized epithelia suggests that apical Ca_i^{2+} signals and apical-to-basal Ca_i^{2+} waves regulate secretion. For example, apical increases in Ca_i^{2+} in pancreatic acinar cells lead to targeting of vesicles to the apical membrane and thus induce exocytosis.[3] Bile ductular secretion depends on apical insertion of water channels[45,46] and other membrane fusion events,[47,48] which establishes a potential role for apical Ca_i^{2+} signals in cholangiocytes. In addition, apical-to-basal Ca_i^{2+} waves direct luminal Cl^- secretion in acinar cells.[3,49] Because Ca_i^{2+} mediates apical bicarbonate secretion in cholangiocytes[33,50] and cholangiocytes express apical, Ca^{2+}-activated Cl^- channels,[51,52] polarized Ca_i^{2+} waves may similarly direct fluid and electrolyte secretion in bile ducts. The small size and intrahepatic location of cholangiocytes limits the ability to relate Ca_i^{2+} signaling to secretion directly in these cells. However, NRC cells are known to form polarized monolayers that exhibit well-defined apical and basolateral domains[21] and have been used to monitor secretion induced by Ca_i^{2+} agonists.[34] Here we furthermore show that the predominant $InsP_3$R in NRC cells is the type III isoform, which is more concentrated apically, and that biliary solutes such as ATP[53] can induce Ca_i^{2+} oscillations in these cells. Thus, the asymmetric distribution of $InsP_3$R isoforms may enable Ca_i^{2+} to regulate secretion by cholangiocytes, and NRC cells seem to be an appropriate model in which to examine this.

Acknowledgments

The authors thank Dr. R. Wojcikiewicz for graciously providing the polyclonal antibodies CT1 and CT2 as well as A. Mennone and M. Lüthi for technical assistance.

Supported by grants from the National Institutes of Health (DK45710, DK57751, TW01451, and DK34989), the Cystic Fibrosis Foundation, and the American Heart Association (to M.H.N.); Swiss National Foundation grant 3100-063696.00 (to J.-F.D.); Swiss National Foundation grant 3234055037.98 (to M.V.S.); and grants from Association pour la Recherche sur le Cancer (6551) and INSERM (contrat PRISME 98-09) (to D.C.).

Abbreviations

Ca_i^{2+}	cytosolic Ca^{2+}
$InsP_3$	inositol 1,4,5-trisphosphate
IP_3R	inositol 1,4,5-trisphosphate receptor
RyR	ryanodine receptor
NRC	normal rat cholangiocyte
ACh	acetylcholine
ATP	adenosine triphosphate
PCR	polymerase chain reaction
RT	reverse transcription
DiD	1,1′-dioctadecyl-3,3,3′,3′-tetramethylindodicarbocyanine perchlorate
mRNA	messenger RNA

References

1. Fernandez-Chacon R, Konigstorfer A, Gerber S, Garcia J, Matos M, Stevens C, Brose N, et al. Synaptotagmin I functions as a calcium regulator of release probability. Nature 2001;410:41–49. [PubMed: 11242035]
2. Cheek TR, Jackson TR, O'Sullivan AJ, Moreton RB, Berridge MJ, Burgoyne RD. Simultaneous measurements of cytosolic calcium and secretion in single bovine adrenal chromaffin cells by fluorescent imaging of fura-2 in cocultured cells. J Cell Biol 1989;109:1219–1227. [PubMed: 2768340]
3. Ito K, Miyashita Y, Kasai H. Micromolar and submicromolar Ca^{2+} spikes regulating distinct cellular functions in pancreatic acinar cells. EMBO J 1997;16:242–251. [PubMed: 9029145]
4. Gomez TM, Spitzer NC. In vivo regulation of axon extension and path-finding by growth-cone calcium transients. Nature 1999;397:350–355. [PubMed: 9950427]
5. Zheng JQ. Turning of nerve growth cones induced by localized increases in intracellular calcium ions. Nature 2000;403:89–93. [PubMed: 10638759]
6. Hahn K, DeBiasio R, Taylor DL. Patterns of elevated free calcium and calmodulin activation in living cells. Nature 1992;359:736–738. [PubMed: 1436037]
7. Lee J, Ishihara A, Oxford G, Johnson B, Jacobson K. Regulation of cell movement is mediated by stretch-activated calcium channels. Nature 1999;400:382–386. [PubMed: 10432119]
8. Dolmetsch RE, Xu K, Lewis RS. Calcium oscillations increase the efficiency and specificity of gene expression. Nature 1998;392:933–936. [PubMed: 9582075]
9. Li W, Llopis J, Whitney M, Zlokarnik G, Tsien RY. Cell-permeant caged InsP3 ester shows that Ca^{2+} spike frequency can optimize gene expression. Nature 1998;392:936–941. [PubMed: 9582076]
10. Maruyama Y, Inooka G, Li YX, Miyashita Y, Kasai H. Agonist-induced localized Ca^{2+} spikes directly triggering exocytotic secretion in exocrine pancreas. EMBO J 1993;12:3017–3022. [PubMed: 8344243]
11. Nathanson MH, Burgstahler AD, Mennone A, Boyer JL. Characterization of cytosolic Ca^{2+} signaling in rat bile duct epithelia. Am J Physiol 1996;271:G86–G96. [PubMed: 8760111]
12. Nathanson MH, Burgstahler AD, Fallon MB. Multi-step mechanism of polarized Ca^{2+} wave patterns in hepatocytes. Am J Physiol 1994;267:G338–G349. [PubMed: 7943230]

13. Giannini G, Conti A, Mammarella S, Scrobogna M, Sorrentino V. The ryanodine receptor/calcium channel genes are widely and differentially expressed in murine brain and peripheral tissues. J Cell Biol 1995;128:893–904. [PubMed: 7876312]
14. Bennett DL, Cheek TR, Berridge MJ, De Smedt H, Parys JB, Missiaen L, Bootman MD. Expression and function of ryanodine receptors in nonexcitable cells. J Biol Chem 1996;271:6356–6362. [PubMed: 8626432]
15. Leite MF, Dranoff JA, Gao L, Nathanson MH. Expression and subcellular localization of the ryanodine receptor in rat pancreatic acinar cells. Biochem J 1999;337:305–309. [PubMed: 9882629]
16. Verma V, Carter C, Keable S, Bennett D, Thorn P. Identification and function of type-2 and type-3 ryanodine receptors in gut epithelial cells. Biochem J 1996;319:449–454. [PubMed: 8912680]
17. Hagar RE, Burgstahler AD, Nathanson MH, Ehrlich BE. Type III InsP3 receptor channel stays open in the presence of increased calcium. Nature 1998;396:81–84. [PubMed: 9817204]
18. Ramos-Franco J, Fill M, Mignery GA. Isoform-specific function of single inositol 1,4,5-trisphosphate receptor channels. Biophys J 1998;75:834–839. [PubMed: 9675184]
19. Bezprozvanny I, Watras J, Ehrlich BE. Bell-shaped calcium-response curves of Ins(1,4,5)P_3- and calcium-gated channels from endoplasmic reticulum of cerebellum. Nature 1991;351:751–754. [PubMed: 1648178]
20. Sonnleitner A, Conti A, Bertocchini F, Schindler H, Sorrentino V. Functional properties of the ryanodine receptor type 3 (RyR3) Ca^{2+} release channel. EMBO J 1998;17:2790–2798. [PubMed: 9582272]
21. Vroman B, LaRusso NF. Development and characterization of polarized primary cultures of rat intrahepatic bile duct epithelial cells. Lab Invest 1996;74:303–313. [PubMed: 8569194]
22. Mignery GA, Sudhof TC, Takei K, De Camilli P. Putative receptor for inositol 1,4,5-trisphosphate similar to ryanodine receptor. Nature 1989;342:192–195. [PubMed: 2554146]
23. Wojcikiewicz RJH. Type I, II, and III inositol 1,4,5-trisphosphate receptors are unequally susceptible to down-regulation and are expressed in markedly different proportions in different cell types. J Biol Chem 1995;270:11678–11683. [PubMed: 7744807]
24. Laemmli UK. Cleavage of structural proteins during the assembly of the head of bacteriophage T_4. Nature 1970;227:680–685. [PubMed: 5432063]
25. Hirata K, Nathanson MH, Burgstahler AD, Okazaki K, Mattei E, Sears ML. Relationship between inositol 1,4,5-trisphosphate receptor isoforms and subcellular Ca^{2+} signaling patterns in nonpigmented ciliary epithelia. Invest Ophthalmol Vis Sci 1999;40:2046–2053. [PubMed: 10440260]
26. Schlosser SF, Burgstahler AD, Nathanson MH. Isolated rat hepatocytes can signal to other hepatocytes and bile duct cells by release of nucleotides. Proc Natl Acad Sci U S A 1996;93:9948–9953. [PubMed: 8790437]
27. Chomczynski P, Sacchi N. Single-step method of RNA isolation by acid guanidinium thiocyanate-phenol-chloroform extraction. Anal Biochem 1987;162:156–159. [PubMed: 2440339]
28. Dufour J-F, Luthi M, Forestier M, Magnino F. Expression of inositol 1,4,5-trisphosphate receptor isoforms in rat cirrhosis. Hepatology 1999;30:1018–1026. [PubMed: 10498655]
29. Hirata K, Nathanson MH, Sears ML. Novel paracrine signaling mechanism in the ocular ciliary epithelium. Proc Natl Acad Sci U S A 1998;95:8381–8386. [PubMed: 9653195]
30. Nathanson MH, Padfield PJ, O'Sullivan AJ, Burgstahler AD, Jamieson JD. Mechanism of Ca^{2+} wave propagation in pancreatic acinar cells. J Biol Chem 1992;267:18118–18121. [PubMed: 1517244]
31. Grynkiewicz G, Poenie M, Tsien RY. A new generation of Ca^{+} indicators with greatly improved fluorescence properties. J Biol Chem 1985;260:3440–3450. [PubMed: 3838314]
32. Blondel O, Takeda J, Janssen H, Seino S, Bell GI. Sequence and functional characterization of a third inositol trisphosphate receptor subtype, IP3R-3, expressed in pancreatic islets, kidney, gastrointestinal tract, and other tissues. J Biol Chem 1993;268:11356–11363. [PubMed: 8388391]
33. Dranoff JA, Masyuk AI, Kruglov EA, LaRusso NF, Nathanson MH. Polarized expression and function of P2Y ATP receptors in rat bile duct epithelia. Am J Physiol 2001;281:G1059–G1067.
34. Schlenker T, Romac J, Sharara AI, Roman RM, Kim S, LaRusso NF, Liddle R, et al. Regulation of biliary secretion through apical purinergic receptors in cultured rat cholangiocytes. Am J Physiol 1997;273:G1108–G1117. [PubMed: 9374709]

35. Nathanson MH. Cellular and subcellular calcium signaling in gastrointestinal epithelium. Gastroenterology 1994;106:1349–1364. [PubMed: 8174894]
36. Leite, MF.; Nathanson, MH. Calcium signaling in the hepatocyte.. In: Arias, IM., editor. The Liver: Biology and Pathobiology. 4th ed.. Raven; Philadelphia: 2001.
37. Leite MF, Burgstahler AD, Nathanson MH. Ca^{2+} waves require sequential activation of inositol 1,4,5-trisphosphate receptors and ryanodine receptors in pancreatic acinar cells. Gastroenterology 2002;122:415–427. [PubMed: 11832456]
38. Allbritton NL, Meyer T, Stryer L. Range of messenger action of calcium ion and inositol 1, 4,5-trisphosphate. Science 1992;258:1812–1815. [PubMed: 1465619]
39. Marchant JS, Parker I. Role of elementary Ca^{2+} puffs in generating repetitive Ca^{2+} oscillations. EMBO J 2001;20:65–76. [PubMed: 11226156]
40. Yule DI, Ernst SA, Ohnishi H, Wojcikiewicz RJH. Evidence that zymogen granules are not a physiologically relevant calcium pool — defining the distribution of inositol 1,4,5-trisphosphate receptors in pancreatic acinar cells. J Biol Chem 1997;272:9093–9098. [PubMed: 9083036]
41. Nathanson MH, Fallon MB, Padfield PJ, Maranto AR. Localization of the type 3 inositol 1,4,5-trisphosphate receptor in the Ca^{2+} wave trigger zone of pancreatic acinar cells. J Biol Chem 1994;269:4693–4696. [PubMed: 7508924]
42. Lee MG, Xu X, Zeng WZ, Diaz J, Wojcikiewicz RJH, Kuo TH, Wuytack F, et al. Polarized expression of Ca^{2+} channels in pancreatic and salivary gland cells — correlation with initiation and propagation of $[Ca^{2+}]_i$ waves. J Biol Chem 1997;272:15765–15770. [PubMed: 9188472]
43. Kasai H, Li YX, Miyashita Y. Subcellular distribution of Ca^{2+} release channels underlying Ca^{2+} waves and oscillations in exocrine pancreas. Cell 1993;74:669–677. [PubMed: 8395348]
44. Thorn P, Lawrie AM, Smith PM, Gallacher DV, Petersen OH. Local and global cytosolic Ca^{2+} oscillations in exocrine cells evoked by agonists and inositol trisphosphate. Cell 1993;74:661–668. [PubMed: 8395347]
45. Marinelli RA, Pham L, Agre P, LaRusso NF. Secretin promotes osmotic water transport in rat cholangiocytes by increasing aquaporin-1 water channels in plasma membrane. Evidence for a secretin-induced vesicular translocation of aquaporin-1. J Biol Chem 1997;272:12984–12988. [PubMed: 9148905]
46. Roberts SK, Yano M, Ueno Y, Pham L, Alpini G, Agre P, LaRusso NF. Cholangiocytes express the aquaporin CHIP and transport water via a channel-mediated mechanism. Proc Natl Acad Sci U S A 1994;91:13009–13013. [PubMed: 7528928]
47. Tietz PS, Alpini G, Pham LD, LaRusso NF. Somatostatin inhibits secretin-induced ductal hypercholeresis and exocytosis by cholangiocytes. Am J Physiol 1995;269:G110–G118. [PubMed: 7631787]
48. Kato A, Gores GJ, LaRusso NF. Secretin stimulates exocytosis in isolated bile duct epithelial cells by a cyclic AMP-mediated mechanism. J Biol Chem 1992;267:15523–15529. [PubMed: 1322400]
49. Kasai H, Augustine GJ. Cytosolic Ca^{2+} gradients triggering unidirectional fluid secretion from exocrine pancreas. Nature 1990;348:735–738. [PubMed: 1701852]
50. Hirata K, Nathanson MH. Bile duct epithelia regulate biliary bicarbonate excretion in normal rat liver. Gastroenterology 2001;121:396–406. [PubMed: 11487549]
51. Fitz JG, Basavappa S, McGill J, Melhus O, Cohn JA. Regulation of membrane chloride currents in rat bile duct epithelial cells. J Clin Invest 1993;91:319–328. [PubMed: 7678606]
52. McGill J, Basavappa S, Mangel AW, Shimokura GH, Middleton JP, Fitz JG. Adenosine triphosphate activates ion permeabilities in biliary epithelial cells. Gastroenterology 1994;107:236–243. [PubMed: 8020667]
53. Chari RS, Schutz SM, Haebig JE, Shimokura GH, Cotton PB, Fitz JG, Meyers WC. Adenosine nucleotides in bile. Am J Physiol 1996;270:G246–G252. [PubMed: 8779965]

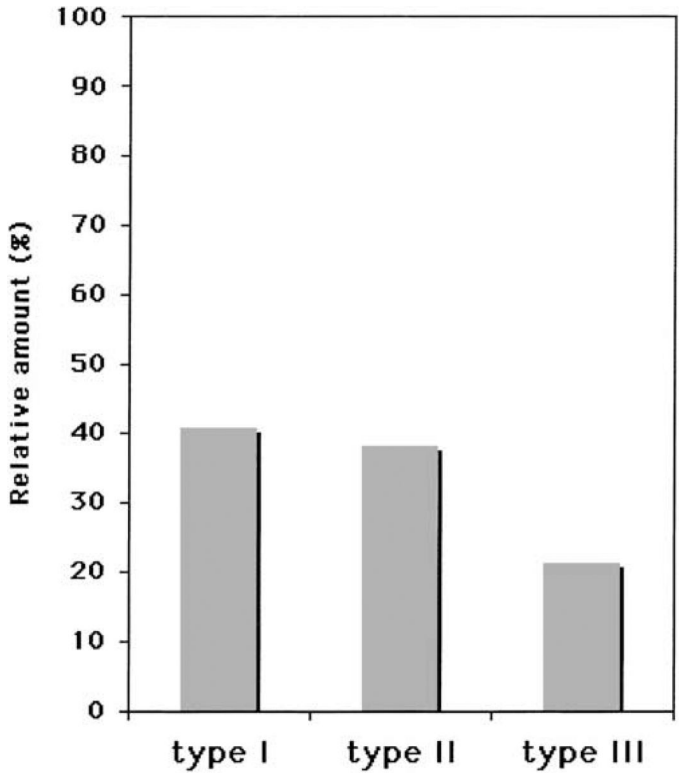

Fig. 1.

$InsP_3R$ isoforms in cholangiocytes measured by real-time quantitative PCR using primers and probes specific for each isoform. Each of the 3 $InsP_3R$ isoforms was expressed; 40.8% of the $InsP_3$ receptor mRNA was for the type I isoform, 38.0% was for type II, and 21.2% was for type III.

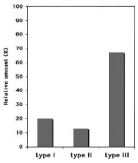

Fig. 2.

$InsP_3R$ isoforms in NRC cells measured by real-time quantitative PCR. Examination of the relative mRNA distribution for each $InsP_3$ receptor isoform showed that the type III isoform is most abundant in NRC cells, representing 67%. Isoforms I and II represented 20% and 13%, respectively.

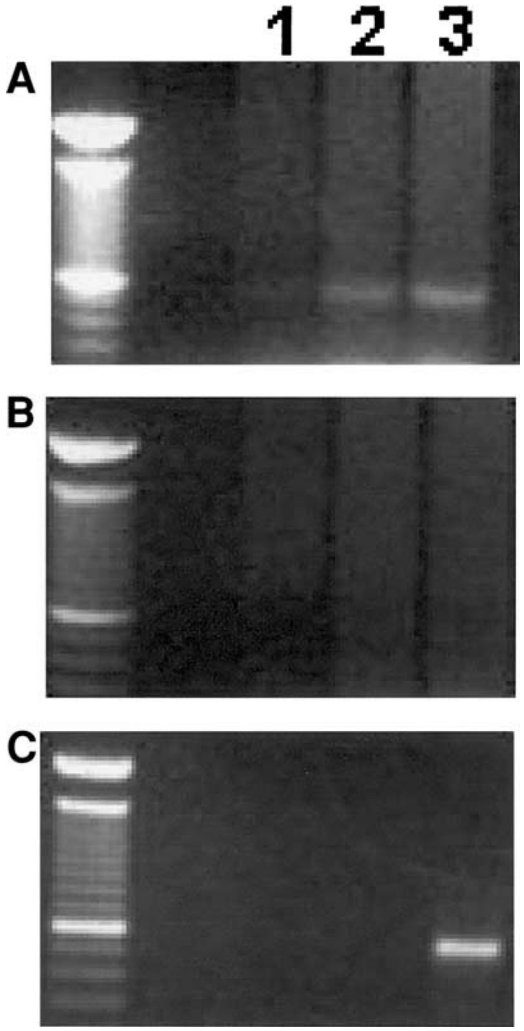

Fig. 3.

RT-PCR fails to detect RyR in cholangiocytes. Using isoformspecific primers, a single 530 – base pair product common to all known RyR isoforms was identified in cardiac RNA (positive control) but not in cholangiocyte RNA or in negative controls. (A) Cardiac RNA after (1) 20, (2) 25, or (3) 30 PCR cycles. (B) Cholangiocyte mRNA after (1) 20, (2) 25, or (3) 30 PCR cycles. (C) Control reactions: (1) DNA control, (2) RNA control, and (3) actin band (500 base pairs), showing that the cholangiocyte RNA is intact.

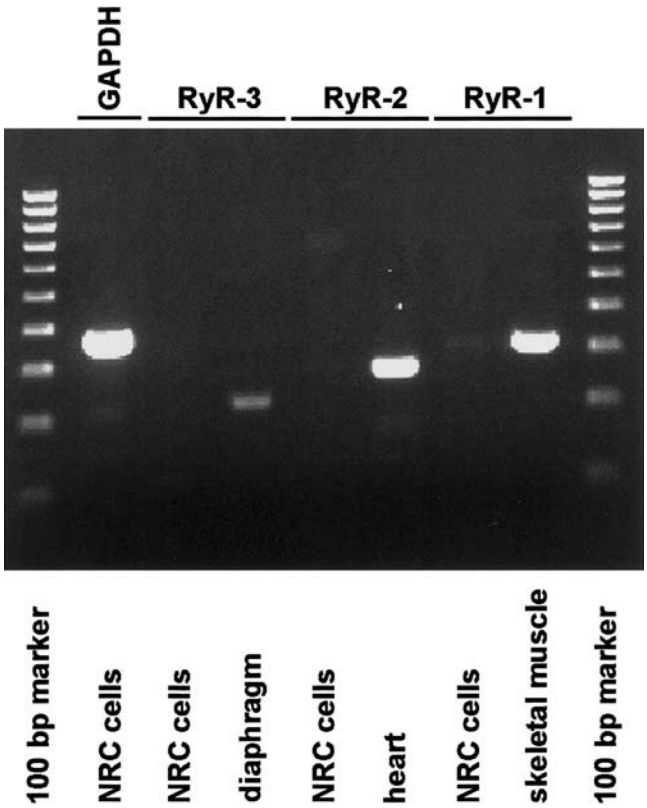

Fig. 4.

RT-PCR assessment of RyR in NRC cells. Using isoform-specific primers, single products were identified in the positive controls, rat skeletal muscle (RyR-1), rat heart (RyR-2), and rat diaphragm (RyR-3). A faint RyR-1 band was seen in NRC cells after 35 PCR cycles, and no band was seen in NRC cells for RyR-2 or RyR-3. A single band is seen for glyceraldehyde-3-phosphate dehydrogenase (GAPDH) in NRC cells, showing that the NRC cell RNA is intact.

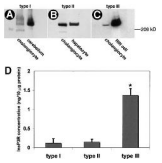

Fig. 5.

Cholangiocytes express all 3 $InsP_3R$ isoforms. (A) Western analysis using a type I–specific $InsP_3R$ antibody identifies a single band of the same size in lysates from cholangiocytes (60 μg) and the positive control, rat cerebellum (8.6 μg). (B) Type II–specific $InsP_3R$ antibody CT2 identifies a single band of the same size in lysates from cholangiocytes and the positive control, rat liver (60 μg each). (C) A monoclonal type III–specific $InsP_3R$ antibody identifies a single band of the same size in lysates from cholangiocytes and the positive control, RIN-5F cells (60 μg each). (D) Quantitative densitometric analysis of $InsP_3R$ isoforms in cholangiocytes. Expression of the type III isoform is significantly greater than either of the other 2 isoforms (*P < .001). Blots were quantified in their linear range, and results are the mean ± SD of n = 5 blots for $InsP_3R$-1, n = 4 for $InsP_3R$-2, and n = 3 for $InsP_3R$-3.

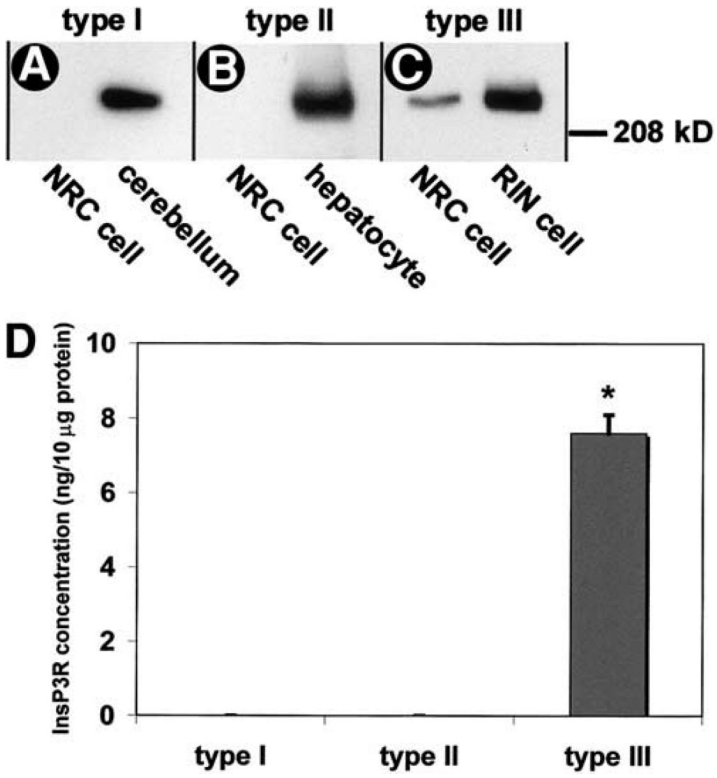

Fig. 6.

NRC cells express only the type III $InsP_3$ receptor. (A) A type I–specific $InsP_3R$ antibody identifies a single band in lysates from the positive control, rat cerebellum (8.6 μg), but not in lysates from NRC cells (40 μg). (B) Type II–specific $InsP_3R$ antibody CT2 identifies a single band in lysates from the positive control, rat liver (60 μg each), but not in NRC cell lysates (40 μg). (C) A monoclonal type III–specific $InsP_3R$ antibody identifies a single band of the same size in lysates from NRC cells (40 μg) and the positive control, RIN-5F cells (60 μg). (D) Densitometric analysis of $InsP_3R$ isoforms in NRC cells. Expression of the type III isoform is greater than the amount observed in cholangiocytes. Blots were quantified in their linear range, and results are the mean ± SD of triplicate blots for each isoform (*$P < .001$).

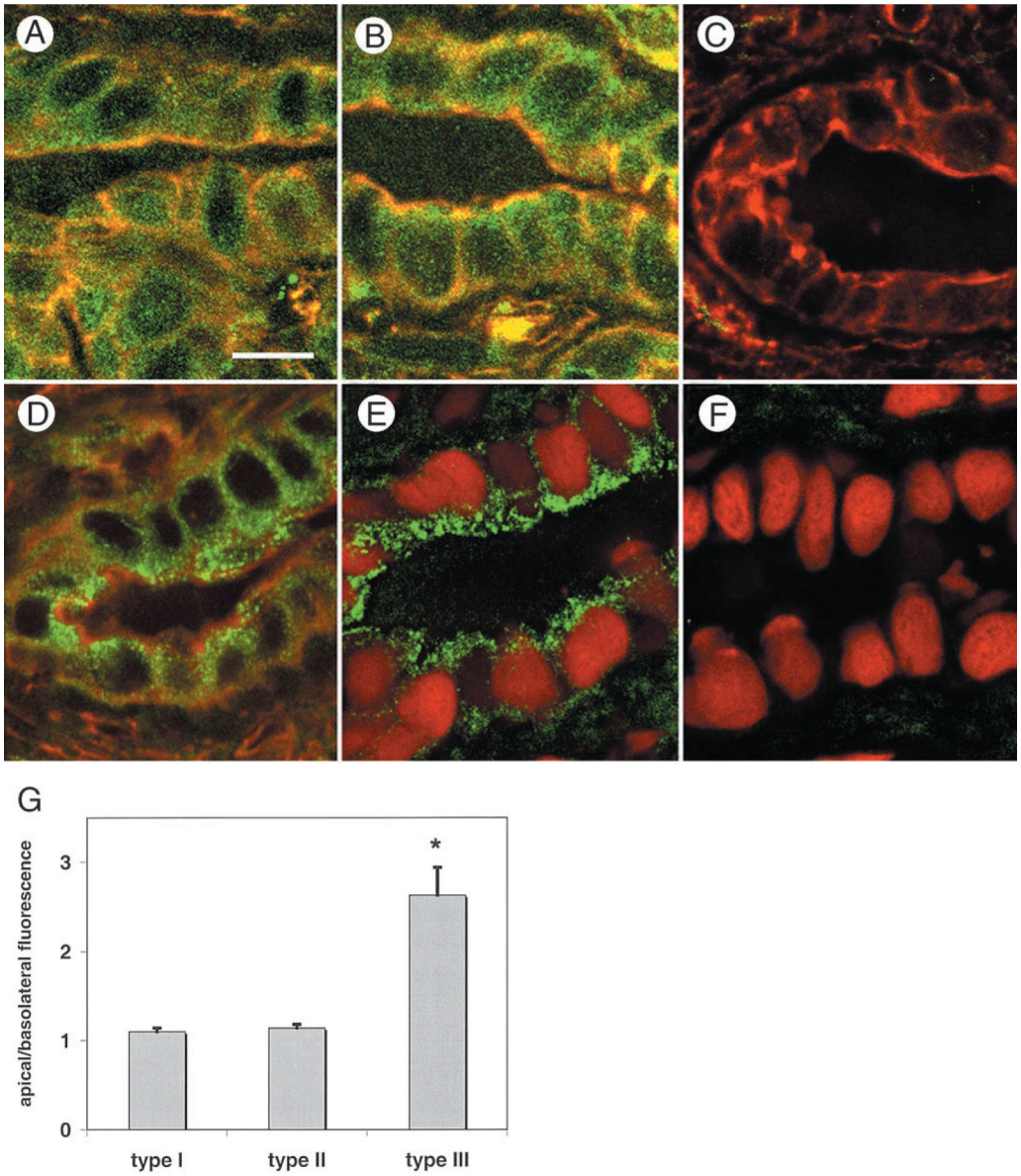

Fig. 7.

Subcellular distributions of $InsP_3R$ isoforms in cholangiocytes as determined by confocal immunofluorescence labeling of rat liver. (A) Distribution of the type I $InsP_3R$ (**green**). The specimen is colabeled with rhodamine-phalloidin (**red**) to identify actin, which outlines the plasma membranes of cholangiocytes. $InsP_3R$ labeling is seen throughout each cholangiocyte. (Scale bar, 10 μm.) (B) Distribution of the type II $InsP_3R$ (**green**) plus rhodamine-phalloidin (**red**) to identify actin, which is predominantly along the plasma membrane. Labeling of this isoform is also seen throughout each cholangiocyte. (C) Double-labeled image of a separate liver section stained with rhodamine-phalloidin (**red**) plus the anti-rabbit secondary antibody used to counterstain the primary antibodies for the type I and type II $InsP_3R$ (**green**). The lack of nonspecific staining by the secondary antibody is evident. (D) Distribution of the type III $InsP_3R$(**green**) plus rhodamine-phalloidin (**red**) to identify actin, which is near the plasma membrane. Labeling of this isoform is diffusely distributed throughout the cytosol but is most intense along the apical membrane of the cholangiocyte. (E) Distribution of the type III $InsP_3R$ (**green**) plus propidium iodide (**red**) to identify the nucleus. This double-labeled image

also shows that the type III $InsP_3R$ is most concentrated near the apical membrane. (F) Double-labeled image of a separate liver section stained with propidium iodide (**red**) plus the anti-mouse secondary antibody used to counterstain the primary antibody for the type III $InsP_3R$ (**green**). The lack of nonspecific staining by this secondary antibody is evident as well. (G) Quantification of $InsP_3R$ immunofluorescence. For each isoform, apical and basolateral immunofluorescence was quantified and the ratio was obtained. The apical and basolateral regions are labeled to a similar extent for both the type I and type II $InsP_3R$, but fluorescence labeling is more than twice as intense in the apical region than in the basolateral region for the type III receptor (*$P < .0002$).

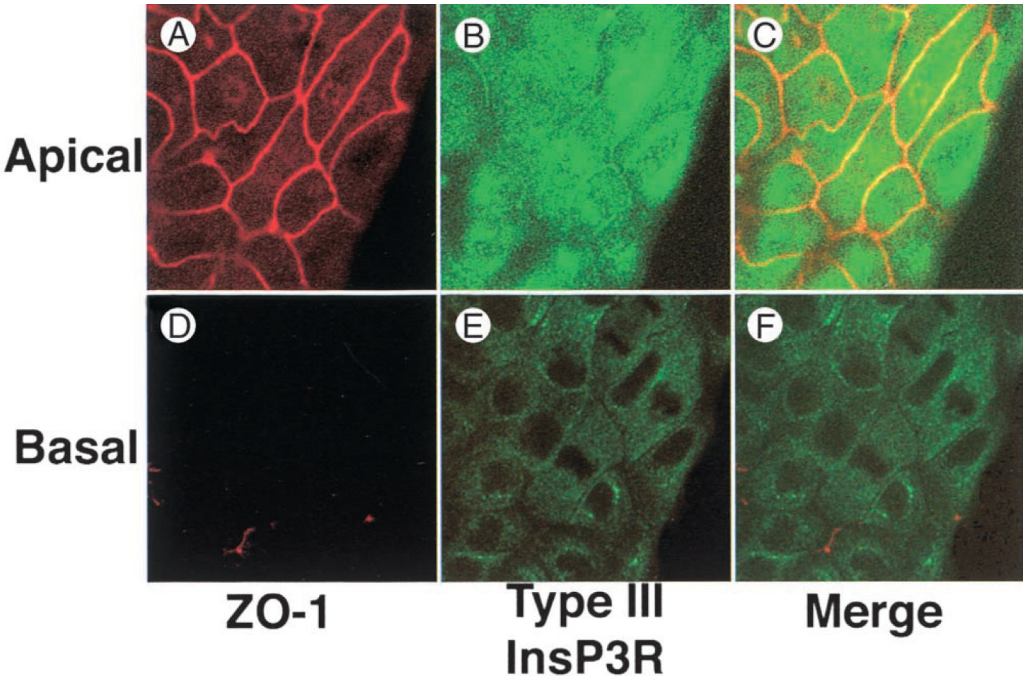

Fig. 8.

Subcellular distribution of the type III $InsP_3R$ in NRC cells as determined by confocal immunofluorescence. Optical sections were obtained in NRC monolayers double labeled with antibodies directed against the type III $InsP_3R$ (**green**) and the tight junction protein ZO-1 (**red**), which identifies the apical region. Type III $InsP_3R$ staining is both intense and diffusely distributed in optical sections near (A-C) the apical membrane but is minimal in optical sections near (D-F) the basolateral membrane.

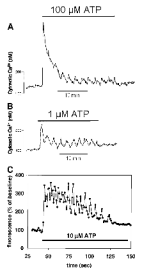

Fig. 9.

Ca^{2+} oscillations in (A and B) NRC cells and (C) cholangiocytes. NRC cells were loaded with fura-2 and then exposed apically to ATP and examined by fluorescence microscopy, whereas cholangiocytes were loaded with fluo-4 and then exposed basolaterally to ATP and examined by confocal microscopy. (A) ATP (100 μmol/L) triggered a large increase in Ca_i^{2+} followed by Ca_i^{2+} oscillations. The Ca_i^{2+} signal stopped with removal of the agonist. (B) A lower concentration of ATP (1 μmol/L) elicited only a small initial increase in Ca_i^{2+}, but this was followed by Ca_i^{2+} oscillations of the same magnitude and frequency as induced by 100 μmol/L ATP. (C) ATP (10 μmol/L) also induces Ca_i^{2+} oscillations in cholangiocytes. This tracing was obtained by monitoring a single cholangiocyte within an isolated bile duct unit using confocal microscopy. The result is representative of that seen in 15 cells.

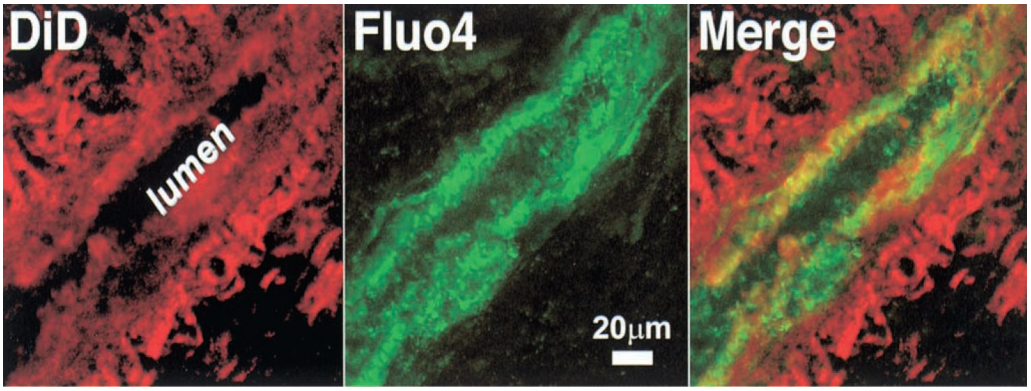

Fig. 10.

Identification of live cholangiocytes within strips of portal tracts. The common bile duct was coinfused with the Ca^{2+} dye fluo-4 and the lipophilic dye DiD, and then strips of portal tracts were isolated and examined by confocal microscopy. The **left panel** shows cholangiocytes and adjacent interstitium stained with DiD. The **middle panel** shows staining with fluo-4 (scale bar, 20 μm). The **right panel** shows the merged (superimposed) image.

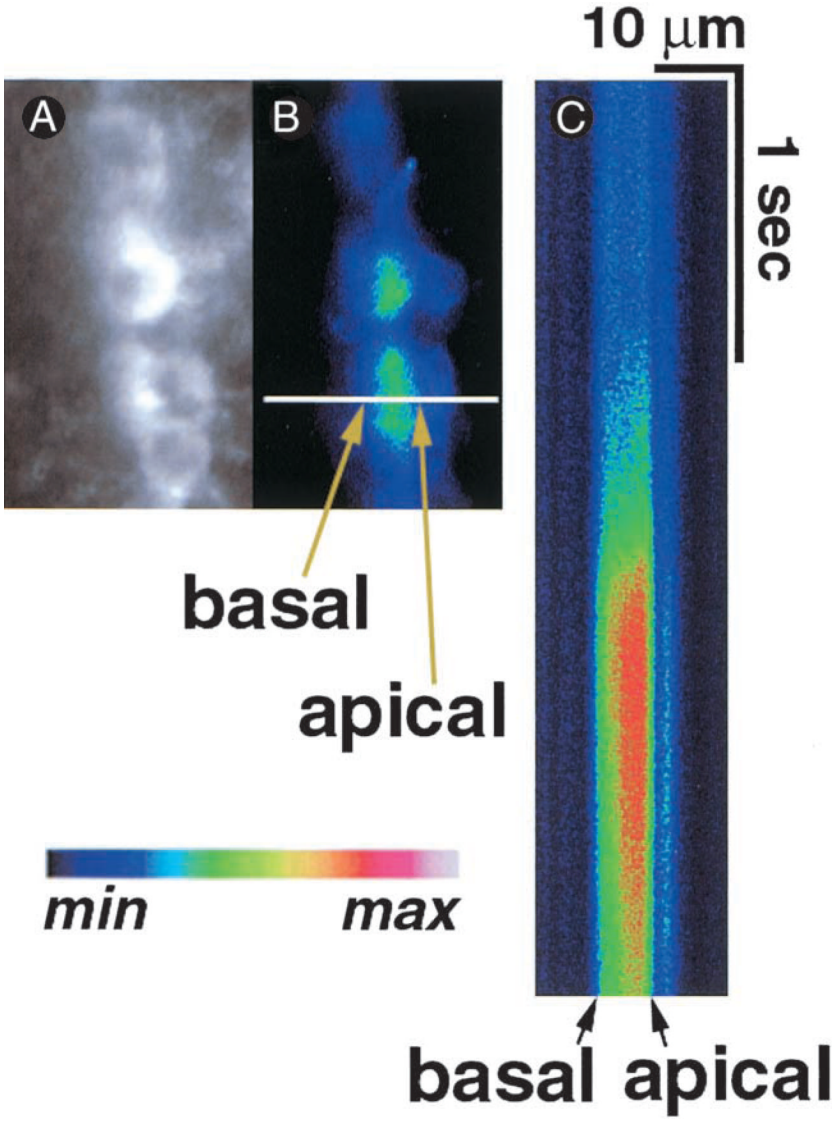

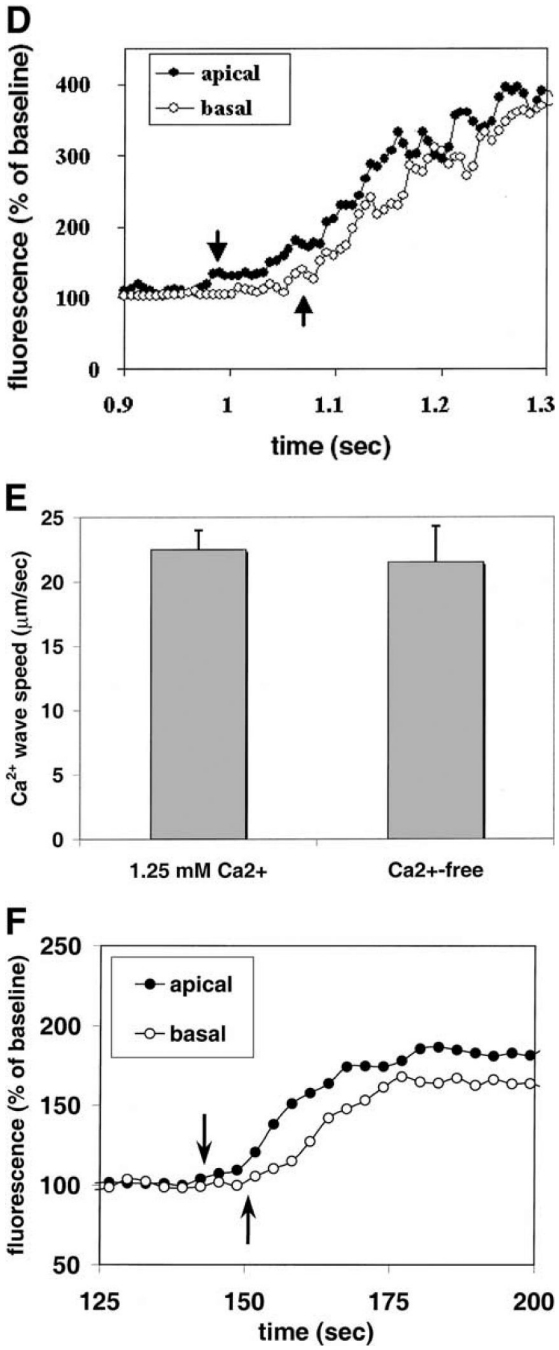

Fig. 11.

ACh-induced Ca_i^{2+} waves in cholangiocytes visualized by confocal line scanning microscopy. (A) Confocal image of a portal tract segment. The cells have been loaded with DiD to facilitate identification. (B) Confocal image of the same segment excited at a lower wavelength to show loading with fluo-4. The line used for line scanning is shown in **white**. Note that the line crosses the apical-to-basal axis of one of the cells. This and the subsequent image are pseudocolored according to the color scale shown below. (C) Confocal line scanning image of the cell shown in B. The tissue was stimulated with ACh (100 μmol/L) as confocal fluorescence along the line was collected every 6 milliseconds. An increase in fluorescence occurs throughout the

cholangiocyte, which begins in the apical region and then spreads rapidly to the basolateral region, representing a Ca_i^{2+} wave that crosses from the apical to the basolateral pole of the cell. (D) Tracing of subcellular Ca_i^{2+} signals in the same cell. The apical increase in Ca_i^{2+} (**left arrow**) precedes the basolateral Ca_i^{2+} increase (**right arrow**) by approximately 100 milliseconds, reflecting an apical-to-basal Ca_i^{2+} wave. Notice that the final increase in Ca_i^{2+} is similar in the apical and basolateral poles, reflecting the fact that the Ca_i^{2+} wave does not diminish as it crosses the cell. The result is representative of that seen in 40 cells. (E) ACh-induced Ca_i^{2+} waves are not affected by extracellular Ca^{2+}. Results are mean ± SEM of 40 cells in Ca^{2+}-containing medium and 8 cells in Ca^{2+}-free medium. (F) Tracing of subcellular Ca_i^{2+} signals in a separate cell stimulated with ATPγS (100 μmol/L). A regenerative, apical-to-basal Ca_i^{2+} wave is seen (**left arrow** indicates onset of apical Ca^{2+} signal, **right arrow** indicates onset of basolateral signal), similar to what is observed in cells stimulated with ACh. The result is representative of that seen in 5 cells.